C-arm Calibration - Is it Really Necessary?*

Ameet Jain[1], Ryan Kon[1], Yu Zhou[2], and Gabor Fichtinger[1,2]

[1] Department of Computer Science, Johns Hopkins University
[2] Department of Mechanical Engineering, Johns Hopkins University

Abstract. C-arm fluoroscopy is modelled as a perspective projection, the parameters of which are estimated through a calibration procedure. It has been universally accepted that precise intra-procedural calibration is a prerequisite for accurate quantitative C-arm fluoroscopy guidance. Calibration, however, significantly adds to system complexity, which is a major impediment to clinical practice. We challenge the status quo by questioning the assumption that precise intra-procedural calibration is really necessary. We derived theoretical bounds for the sensitivity of 3D measurements to mis-calibration. Experimental results corroborated the theory in that mis-calibration in the focal spot by as much as 50 mm still allows for tracking with an accuracy of 0.5 mm in translation and 0.65^o in rotation, and such mis-calibration does not impose any additional error on the reconstruction of small objects.

1 Introduction

C-arm fluoroscopy is ubiquitous in general surgery, due to its real-time nature, versatility, and low cost. At the same time, quantitative fluoroscopy has not found a *large scale clinical acceptance*, because of inherent technical difficulties and needs to solve four major problems: (1) C-arm image distortion; (2) Calibration of model parameters; (3) Pose recovery or tracking when multiple images are taken; and (4) Registration to imaging modalities. Some of the prominent works that have tackled the above problems are [1, 2]. The driving application of our research is prostate brachytherapy, where radioactive seeds are required to be precisely placed into the prostate. Quantitative fluoroscopy could enable a significant improvement in the current clinical practice.

If is known that both image distortion[3] and calibration[4] may vary significantly with pose. Image distortion usually has a consequential contribution to reconstruction error and needs to be compensated. Thus the additional cost of a full online calibration is not substantial. Recently developed advanced intensifier tubes allow for lesser distortion, while modern flat panel detectors obviate distortion correction altogether. This fact brings up the question whether we need to calibrate the C-arm fully at each pose. The question also leads to the broader issue, that even if it is not pose dependent, how accurate does calibration need to be. In spite of the importance of calibration in C-arm fluoroscopy, as far as the authors are aware, there has been no prior work that conducts this analysis. The

* This work has been supported by NIH 1R43CA099374-01 and NSF EEC-9731478.

J. Duncan and G. Gerig (Eds.): MICCAI 2005, LNCS 3749, pp. 639–646, 2005.
© Springer-Verlag Berlin Heidelberg 2005

vision community has a similar problem [5, 6] when cameras are used for visual serving of robots. We do not go into a detailed comparison for lack of space.

In quantitative C-arm fluoroscopy, we typically need to measure the spatial transformation between two objects, such as a vertebra and a bone drill, as compared to the transformation between an object and the C-arm itself. Thus the central intuition of this paper is that *while an incorrect calibration gives erroneous estimates for the absolute transformations, nevertheless it still provides acceptable relative estimates.* The consequence of this conjecture is potentially far reaching, as it can turn fluoroscopy to an affordable quantitative measurement tool in a large family of procedures. It should be however noted that we do not claim that calibration would always be unnecessary, since there are many applications that require high reconstruction accuracy. The decision should always be made case by case, experimentally. In this paper, we build a mathematical framework to formally address this issue and lend credit to the intuition that a loose estimate of the C-arm parameters might suffice in applications where the relative pose of objects is to be measured. In particular, we prove in theory and demonstrate experimentally that intra-operative dosimetry of brachytherapy implants is feasible with an un-calibrated C-arm.

2 Mathematical Framework

C-arm Imaging Model: Geometric aspects of fluoroscopic imaging can be approximated as a perspective projection with five parameters[7]. There are a total of five independent parameters that need to be evaluated by the calibration procedure - the pixel sizes (two) and the focal spot (three). The pixel sizes are fixed and remain unchanged throughout the life of the C-arm, reducing online-calibration to just the focal spot. Though our framework can study sensitivity due to any of the five parameters, we limit ourselves only to the focal spot.

2.1 Model for Reconstruction Space Transformation

As illustrated in Figure 1(a), let A & B (with reference frames F_A & F_B) be the two objects being imaged. The assumptions are: (i) ${}^{I}F_A$,${}^{I}F_B$ can be computed from the images; (ii) A & B are *not large* in comparison to the focal length; (iii) F_A and F_B are *close by*; and (iv) the quantity of interest is ${}^{A}F_B = ({}^{I}F_A)^{-1}\,{}^{I}F_B$. Let $\bar{f}_1$ be the true focal spot and $\bar{f}_2 = (\bar{f}_1 + \bar{D})$ be the mis-calibrated estimate. We claim that even though the absolute locations of the objects are off, their relative transformation might still be accurate.

A transformation is needed that can take the absolute location of an object reconstructed with calibration $\bar{f}_1$, and compute its corresponding location with calibration $\bar{f}_2$. We claim that the simplest transformation will be a linear affine model $\mathcal{T}$. The intuition derives from the observation that the image plane is the same in both reconstruction spaces. Thus if P_1 (not in homogenous coordinates) projects to a point p on the image, then it is constrained to be on line $\bar{L}_1$ in the $\bar{f}_1$-space and on $\bar{L}_2$ in $\bar{f}_2$-space. Thus we seek a continuous invertible

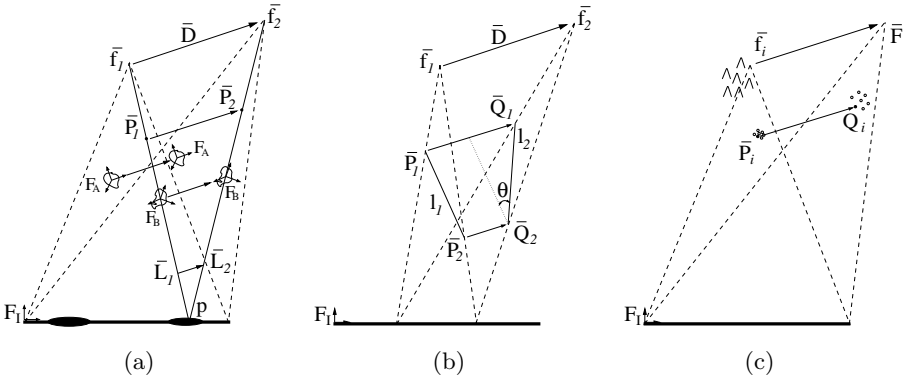

Fig. 1. Mis-calibration (a) shifts all reconstructed objects under an affine transformation; (b) rotates and scales a straight line segment; (c) Pose dependent calibration might be successfully approximated by using the mean value

transformation that projects $\bar{L}_1$ to $\bar{L}_2$. By incorporating the above constraints, $\mathcal{T}$ can be evaluated to be,

$$P_2 \;=\; \mathcal{T} \cdot P_1 \;=\; \begin{bmatrix} 1 & 0 & D_x/f_{1z} \\ 0 & 1 & D_y/f_{1z} \\ 0 & 0 & 1+(D_z/f_{1z}) \end{bmatrix} \cdot P_1 \;=\; P_1 + (d \cdot Z/f_{1z})\hat{D} \quad (1)$$

where with respect to (wrt) F_I, $\bar{D} = (D_x, D_y, D_z)$; $d = \|\bar{D}\|_2$; $\hat{D} = \bar{D}/d$; $\bar{f}_1 = (f_{1x}, f_{1y}, f_{1z})$; and $P_1 = (X, Y, Z)$. Each point is effectively translated in direction $\hat{D}$ by an amount proportional to its distance from the image. Experiments measuring the correctness of this affine model are available in Section 3. Thus to study sensitivity, it is sufficient to study the properties of $\mathcal{T}$.

2.2 Changes in Length and Scale

$\mathcal{T}$ preserves the scale along the x, y-axes, but scales the space along the z-axis. Let $P_1(X_1, Y_1, Z_1)$ & $P_2(X_2, Y_2, Z_2)$ be any two points (not necessarily close to each other) in the $\bar{f}_1$-space at a distance of l_1. $\mathcal{T}$ maps them to points Q_1 & Q_2 in the $\bar{f}_2$-space at a distance of l_2 (Figure 1 (b)). It can be shown that

$$\|l_2 - l_1\| \;\leq\; \frac{d}{f_{1z}}|Z_1 - Z_2| \quad (2)$$

It directly follows from Equation (2) that $\mathcal{T}$ does not alter the length significantly. As an example, a 10 mm calibration error would affect the length of a 30 mm thoracic pedicle screw at an angle of 45^o by less than 0.2 mm (focal length $\sim$ 1 m), which is significantly less than the error from other sources. Thus F_A, F_B will not change their relative translation by a factor more than that specified by Equation (2).

2.3 Changes in Absolute Orientation

A change in orientation results from the object having a depth (Figure 1 (c)). It can be shown geometrically that the orientation error is maximal when the vector $\overline{P_1P_2}$ is roughly orthogonal to $\bar{D}$ and is purely in the vertical plane. The amount (θ) and the axis ($\hat{\kappa}$) of rotation, through a series of computations can be shown to be as in Equation (3). The bound on the rotation error is dependent only on origin mis-calibration and not on that in focal length . More importantly it is independent of the height/depth of the object (as far as it is non-planar) and its distance from the image plane. Thus F_A, F_B in Figure 1 will observe the same absolute rotation, in effect not experiencing any relative rotation. Experimental results corroborating this claim are available in Section 3.

$$|\theta| \leq \arcsin\left[\frac{\sqrt{D_x^2+D_y^2}}{f_{1z}}\right] \sim \frac{\sqrt{D_x^2+D_y^2}}{f_{1z}} \; ; \quad \hat{\kappa} = \frac{1}{\sqrt{D_x^2+D_y^2}}(D_y, -D_x, \; 0) \tag{3}$$

2.4 Error in Reconstruction of Point Features

In many applications (particularly in brachytherapy), C-arms are used to reconstruct 3D point objects. This is done by obtaining multiple images at varying orientations and then using triangulation to obtain the desired intersection. In ideal circumstances, all the lines would intersect at a unique point. In practice however, calibration (and other) errors lead to non-intersecting lines. We will attempt to bound the error in this symbolic reconstruction of the point. Let point P be imaged from N different poses and reconstructed in a tracker frame F_A, which is stationary wrt P. Let the i^{th} pose have a focal spot error (in frame F_A) of $\bar{D}_i$. Without errors, each reconstructed line (l_i) would pass through P. It can be shown that due to the calibration error $\bar{D}_i$, the new line passes through a new point $\bar{P}'_A$ and undergoes a rotation ϕ.

$$\bar{P}'_A \sim \bar{P}_A + [0 \;\; 0 \;\; \frac{(\bar{P}_A \cdot \bar{D}_i)}{f_{iz}}]' \quad ; \qquad \phi \sim \frac{(\hat{l}_i \cdot \bar{D}_i) \; sin\theta_i}{f_{iz}} \tag{4}$$

where θ_i is the angle that l_i makes with the z-axis of F_A. The rotation is fairly small and can be ignored. Thus P_A is at a distance of $(\bar{P}_A \cdot \bar{D}_i)sin\theta_i/f_{iz}$ from l_i. If Q is the symbolic intersection of all l_i's, then it can be shown that Q is no further away than $(\frac{d_{max}}{f_z} sin\theta_{max})\|P_A\|$ away from any of the lines. Moreover, the reconstruction error (RE) can also be shown to be bounded by

$$RE = \|(\bar{Q} - \bar{P}_A)\| < \frac{\sqrt{2} \; d_{max}}{f_z} \; \|\bar{P}_A\| \tag{5}$$

where d_{max} is the maximum amount of mis-calibration and f_z is the minimum focal length. Thus a 10 mm focal length error causes an error less than 0.5 mm for a point at a distance of 35 mm. Note that this is the worst case error analysis and in practice the dot product in Equation (4) mutually cancels positive and negative errors, leading to extremely low reconstruction errors (Section 3).

2.5 The Optimal Choice for Calibration Parameters

Since the focal spot is pose dependant, and the results from Section 2.2, & 2.3 suggest robustness to mis-calibration, choosing a constant calibration for quantitative reconstruction might be viable. In the scenario that the focal spot might vary as much as 10 *mm* from one pose to another, "*what constant calibration should be chosen to minimize error*"?

Let us assume that we are imaging a point P from N different poses (Figure 1 (c)). Wrt frame F_I, let the i^{th} pose have the focal spot at $\bar{f}_i = (f_{ix}, f_{iy}, f_{iz})$ and the point be at location $P_i = (X_i, Y_i, Z_i)$. Note that we assume: (a) variations in each of $f_{ix}, f_{iy}, f_{iz}, X_i, Y_i, Z_i$ & pose are independent; (b) P_i's are close to the iso-center, *i.e.* variations in X_i, Y_i, Z_i are not high. We choose a constant value of $\bar{F} = (F_x, F_y, F_z)$ for the focal spot, which will displace the point P_i to $Q_i = \mathcal{T}(\bar{f}_i, F) \cdot P_i$. The aim is to choose an $\bar{F}$ which minimizes the net variation of $\Delta Q_i = Q_i - \mu_Q$. Through a series of computations, it can be shown that

$$\mu_Q = \mu_P + \frac{\mu_z}{\mu_{fz}}(\bar{F} - \bar{\mu}_f) \tag{6}$$

$$\Delta Q_i = (P_i - \mu_P) + [\frac{\Delta Z_i}{\mu_{fz}} - \frac{\mu_z \Delta f_{iz}}{\mu_{fz}^2}]\bar{F} + \frac{\mu_z \Delta f_{iz}}{\mu_{fz}^2}\bar{\mu}_f - \frac{\Delta Z_i}{\mu_{fz}}\bar{\mu}_f - \frac{\mu_z}{\mu_{fz}}\Delta\bar{f}_i \tag{7}$$

where $\mu_Q, \mu_P, \mu_z, \mu_{fz}, \bar{\mu}_f$ are the mean values of $Q_j, P_j, Z_j, f_{jz}, \bar{f}_j$; $Z_j = \mu_z + \Delta Z_j$ and likewise for $f_{jz}, \bar{f}_j$, where $j = 1 \ldots N$. In the above calculations, the second order terms either summed to 0 due to the independence of the variables or were too small in comparison. Our choice of $\bar{F}$ should be the one that minimizes the $variance(\Delta Q) = var(\Delta Q_x) + var(\Delta Q_y) + var(\Delta Q_z)$. It should be noted that F_z scales the whole space, *i.e.* a lower value will decrease the variance, implying that the choice of $F_z = 0$ forces $var(Q_z) = 0$ by forcing all $Q_i's$ to lie on a plane. Thus $var(Q_z)$ does not provide sufficient constraints for F_z. We will first obtain F_x, F_y by minimizing the variance along x, y-axes (since there is no scaling in these directions), and then will compute F_z. Notice that the first term in Equation (7) is due to the relative movement in P, while the rest is due to an error in the calibration. Since we are interested only in the variance due to mis-calibration, we will ignore the variations in P. Minimizing $var(\Delta Q)$ and enforcing independence of f_{ix}, f_{iy} & f_{iz} gives

$$\bar{F} \;=\; \bar{\mu}_f - \frac{\Sigma_1^N \Delta f_{iz} \Delta \bar{f}_j}{\Sigma_1^N \Delta f_{iz}^2}\,\mu_{fz} \;=\; [\,\mu_{fx},\;\; \mu_{fy},\;\; 0\,]^T \tag{8}$$

As expected, $F_z = 0$ from above. To compute F_z, we need to impose length preserving constraints. Thus if we measure a line segment of length l in each image, use Equation (2) to derive the net length error, the minimization implies

$$F_z \;=\; \mu_{fz}(1 - \frac{\Sigma_1^N \Delta f_{iz}^2}{N\mu_{fz}^2}) \;\sim\; \mu_{fz} \tag{9}$$

Thus $\bar{F} = \bar{\mu}_f$ (the mean), which is fairly intuitive and probably in common practice. Likewise, this particular choice of F_x, F_y is also a length preserving

constraint, *i.e.* it minimizes the error in lengths of line segments. Calibration error in ΔQ_i now reduces to $-\frac{\mu_z}{\mu_{fz}}\Delta\bar{f}_i$, which has a stable mean and low variance. Equation (10) gives a bound on the error when the assumed value of $\bar{F}$ is away from the mean $\bar{\mu}_f$ by a distance d. A 10 mm variation in the focal length ($var \sim 3\ mm$), $P's$ roughly at the iso-center having a depth variation of 100 mm and the assumed calibration unusually away from $\bar{\mu}_f$ by 50 mm still bounds the maximum error by 0.75 mm. Thus large and constant mis-calibration in many applications, might still provide sub-millimetric 3D quantitative measurements.

$$error \quad \leq \quad \frac{\sqrt{d^2 var(Z) + \mu_z^2 var(\|\bar{f}\|)}}{\mu_{fz}} \tag{10}$$

3 Phantom Experiments and Results

Validity of the Model: Equations (1) & (3) give the translation and rotation transformations as predicted by the affine model, the accuracy of which would furnish the validity of the model. We used the FTRAC fiducial (Figure 3), a small image-based fluoroscope tracking fiducial, which (given the calibration) can track a C-arm with an accuracy of 0.5 mm in translation and 0.65^o in rotation [7]. The fiducial was imaged using a Philips Integris V3000 fluoroscope and the true calibration read off the machine display. The images were not corrected for distortion. The pose of the fiducial (wrt to F_I) was first evaluated using the correct calibration, and then with the mis-calibrated parameters. The difference between the pose change predicted by the equations and the one computed using the non-linear pose estimation software, is displayed in Figure 2 (a) as a function of maximum calibration error. Even when mis-calibration is as high as 50 mm, the model can predict the rotation-axis with an accuracy of 4^o, amount of rotation under 1^o and translation under 1.5 mm. For extreme mis-calibrations the translation error linearly increases, while rotation is still stable. Thus the model seems to predict with an acceptable accuracy.

Accuracy of C-arm Tracking: The FTRAC fiducial was mounted on a 0.02^o accuracy rotational turntable, while the fluoroscope was kept stationary. The turntable was rotated by known precise amounts (ground truth) and images were taken. The relative poses were also computed using the pose estimation software. The accuracy in the estimation of C-arm motion is given by the difference between the computed relative pose and the true relative pose. The tracking accuracy is plotted in Figure 2 (b) as a function of mis-calibration. Even a high mis-calibration of 150 mm adds no *additional* error in C-arm motion estimation, fixing the value at 0.45 mm in translation and 0.6^o in rotation. An unusually high mis-calibration of 400 mm also only marginally decreases accuracy. Thus, mis-calibration does not increase the error of C-arm tracking .

3D Quantitative Reconstruction using Multiple Images: In addition to tracking a C-arm, it is equally important that multiple objects in the field of view (eg. vertebrae and screws) be reconstructed accurately relative to each

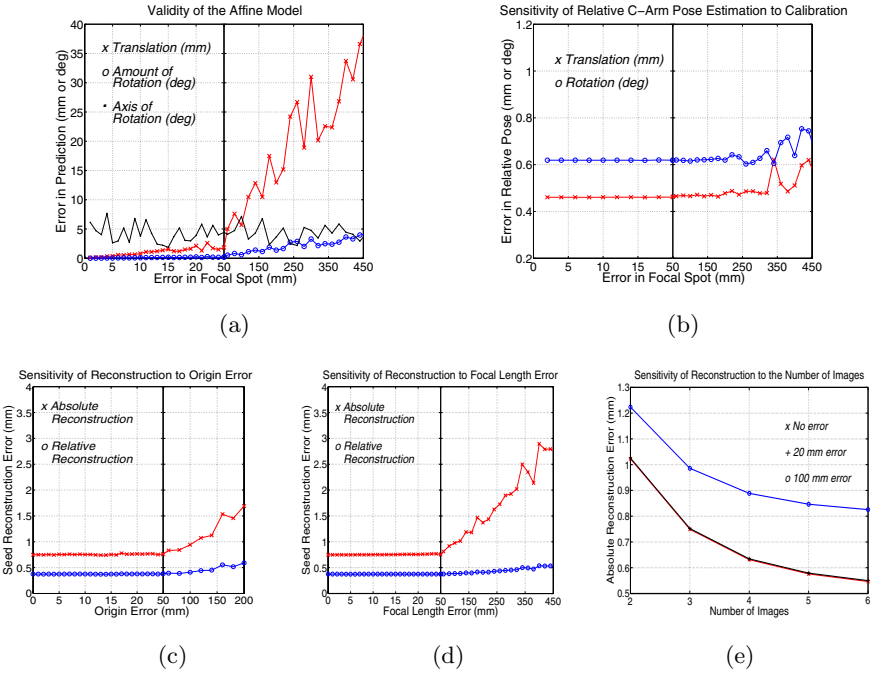

Fig. 2. Note the scale variation in x-axis. (a) An affine transformation is able to predict the movement of 3D objects due to mis-calibration; (b) C-arm tracking is insensitive to mis-calibration; 3D Reconstruction is insensitive to mis-calibration in (c) origin; (d) focal length up to 50 *mm*, beyond which it starts to linearly drift away from the tracking fiducial. Notice that the shape of the implant (relative err) is barely altered; (e) 3D reconstruction error decreases with an increase in images used.

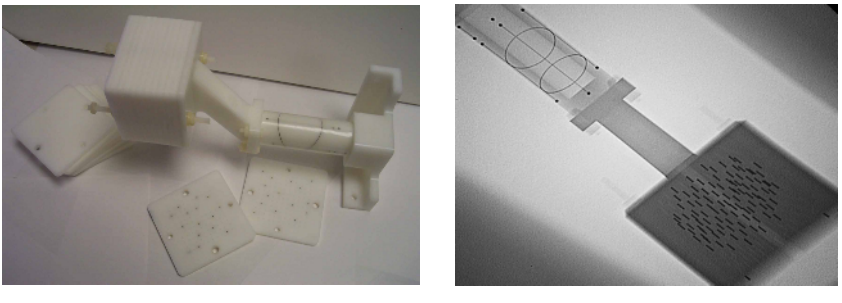

Fig. 3. An image of the seed phantom attached to the FTRAC fiducial (left). The seed phantom can replicate any implant configuration, using the twelve 5 *mm* slabs each with over a hundred holes. A typical X-ray image of the combination (right).

other. In order to validate our hypothesis that 3D reconstruction might not be sensitive to mis-calibration, we use an accurate acetol phantom (Figure 3) having 100 dummy radioactive seeds, approximating a brachytherapy implant

(Figure 3). The true 3D coordinate of each seed wrt the fiducial is known by rigid attachment. The C-arm is tracked using the FTRAC fiducial and the 3D seed coordinates are computed by triangulation (an algorithm called MARSHAL is used to establish correspondences). The difference between the computed and the true seed location gives us the 3D reconstruction error for each seed (wrt fiducial). The relative reconstruction error removes any consistent shift reflecting any change in shape. These errors are plotted as a function of mis-calibration in Figure 2 (c), (d). The reconstruction error is insensitive to mis-calibration in origin and focal length errors of up to 50 mm. The shape of the implant is stable even for large calibration errors. Figure 2 (e) shows a drop in reconstruction error as the number of images increase. Thus mis-calibration does not decrease reconstruction accuracy.

4 Conclusion

We modelled the the effects of mis-calibration on 3D reconstruction as an affine transform, and proved its validity experimentally. We have derived bounds on the amount of scaling, translation and rotation error. For pose dependant calibration, we proved that using the mean calibration minimizes the reconstruction variance. Phantom experiments with a radiographic fiducial indicate that C-arm tracking is insensitive to mis-calibrations. We also showed that mis-calibration up to 50 mm adds no additional error in 3D reconstruction of small objects, beyond which the reconstructed objects begin to drift wrt the fiducial, while still retaining the shape. In conclusion, a significant family of quantitative fluoroscopy applications involving localization of small markers can function without cumbersome on-line calibration. A constant loose calibration might suffice.

References

1. Hofstetter, R., Slomczykowski, M., Sati, M., Nolte, L.: Fluoroscopy as an imaging means for computer-assisted surgical navigation. CAS **4(2)** (1999) 65–76
2. Yao, J., Taylor, R.H., et al: A c-arm fluoroscopy-guided progressive cut refinement strategy using a surgical robot. Comput Aided Surg **5(6)** (2000) 373–90
3. Fahrig, R., et al: Three-dimensional computed tomographic reconstruction using a c-arm mounted XRII: correction of image distortion. Med Phys. (**24(7)**) 1097–106
4. Livyatan, H., Yaniv, Z., Joskowicz, L.: Robust automatic c-arm calibration for fluoroscopy-based navigation: A practical approach. In: MICCAI. (2002) 60–68
5. Kumar, R., Hanson, A.: Sensitivity of the pose refinement problem to accurate estimation of camera parameters. In: ICCV90. (1990) 365–369
6. Malis, E.: Visual servoing invariant to changes in camera intrinsic parameters. IEEE Transaction on Robotics and Automation **20** (2004) 72–81
7. Jain, et al: A robust fluoroscope tracking (FTRAC) fiducial. In: SPIE Medical Imaging; Visualization, Image-Guided Procedures & Display. (2005) 798–809